



**HAL**  
open science

## Response regimes of a cutting tool on a lathe strongly coupled to a nonlinear energy sink

Etienne Gourc, Sébastien Seguy, Guilhem Michon, Alain Berlioz

### ► To cite this version:

Etienne Gourc, Sébastien Seguy, Guilhem Michon, Alain Berlioz. Response regimes of a cutting tool on a lathe strongly coupled to a nonlinear energy sink. XVIIIth Symposium Vibrations, SHocks & NOise VISHNO, 3-5 juillet 2012, Paris, France, Jul 2012, Paris, France. hal-02186319

**HAL Id: hal-02186319**

**<https://hal.science/hal-02186319v1>**

Submitted on 1 Jul 2021

**HAL** is a multi-disciplinary open access archive for the deposit and dissemination of scientific research documents, whether they are published or not. The documents may come from teaching and research institutions in France or abroad, or from public or private research centers.

L'archive ouverte pluridisciplinaire **HAL**, est destinée au dépôt et à la diffusion de documents scientifiques de niveau recherche, publiés ou non, émanant des établissements d'enseignement et de recherche français ou étrangers, des laboratoires publics ou privés.

Vibrations, Shocks and Noise

# Response regimes of a cutting tool on a lathe strongly coupled to a nonlinear energy sink

E. Gourc<sup>a\*</sup>, S. Seguy<sup>a</sup>, G. Michon<sup>b</sup>, A. Berlioz<sup>c</sup>

<sup>a</sup>Université de Toulouse, ICA, INSA, 31077 Toulouse, France

<sup>b</sup>Université de Toulouse, ICA, ISAE, 31055 Toulouse, France

<sup>c</sup>Université de Toulouse, ICA, UPS, 31062 Toulouse, France

---

## Abstract

This paper investigates the different response regimes of a cutting tool on a lathe strongly coupled to a Nonlinear Energy Sink (NES). The system consists of a linear oscillator representing a flexible lathe tool, subject to a regenerative cutting force and strongly coupled to a NES. The linear part of the cutting force is considered. The equations of motion are analyzed via the method of multiple scales. Condition of elimination of secular terms permit to derive equation of the slow invariant manifold (SIM) and the behavior of the system has been explained by studying the location of the fixed points of the slow flow on the SIM. Different types of responses are revealed such as periodic response and also Strongly Modulated Response (SMR) that are not related to the fixed points of the slow flow. Analytic results are then compared with numerical simulations. The potential benefit of the NES to control machining chatter is demonstrated. It should be interesting to include a non-linear cutting law, and to study the system behavior for a larger set of parameters and an optimized NES.

Keywords: dynamic ; turning ; chatter ; Nonlinear Energy Sink

---

## 1. Introduction

Surface quality of parts produced by machining operation is strongly affected by the well-known regenerative chatter. The chatter instability is induced by the time delay between two consecutive workpiece revolution. By the effect of some external disturbance, the tool start damped oscillations relative to the workpiece, and the surface roughness is undulated. For two consecutive workpiece revolutions, the chip thickness is modulated. This regenerative mechanism was presented first by Tobias [1]. Since this work, many researchers have improved the knowledge by the stability lobe representation, see e.g. [2, 3]. The behavior of a cutting tool on a lathe has also been studied using the method of multiple scales [4].

Various techniques for chatter suppression have been investigated. In [5], a variable spindle speed in milling to disturb the time delay was used. Another approach to reduce chatter is the use of linear tuned vibration absorbers. Recently, an analytical optimized method was presented for linear absorbers in the context of chatter [6]. These linear absorbers are successfully applied on boring process [7]. Active absorbers have been also proposed with piezoelectric tool [8]. However all these linear absorbers are limited by the small frequency bandwidth, and in practice their efficiency is not interesting for the machinist.

The idea of attaching a nonlinear oscillator to a turning machine is relatively new [9]. In recent studies, it has been demonstrated that addition of a small mass attachment with a strong nonlinear coupling (i.e. a Nonlinear Energy Sink) to a linear oscillator can be benefit for vibration mitigation [10, 11]. In [12], a general analytical

---

\* Corresponding author. Tel.: +33 561 559 222; fax: +33 561 559 950.  
E-mail address: gourc@insa-toulouse.fr.

procedure was presented. The possibility to control self-excitation regimes in a Van der Pol oscillator with a NES has been demonstrated in [13]. Systems with NES exhibit regimes that are not related to fixed points, and cannot be explained using local analysis [14]. These regimes are related to relaxation oscillations of the slow flow and are also interesting for passive control.

In this paper, the possibility of controlling regenerative chatter using a nonlinear energy sink is analyzed for turning process. Theoretical predictions are compared with numerical integration. In the next section, the model considered is described. In the third section, the asymptotic analysis of the equation of motion is performed. Then, different response regimes accompanied with numerical simulation are presented.

## 2. Mechanical model

The model studied herein consists in a lathe cutting tool with an embedded NES. Only the first flexible mode of the cutting tool is considered, and the workpiece is assumed to be rigid. A schematic of the model is proposed in Fig. 1 and the governing equation of motion are:

$$m_1 \ddot{x} + c_1 \dot{x} + k_1 x + c_2 (\dot{x} - \dot{y}) + k_2 (x - y)^3 = F(\Delta h(t)) \quad (1)$$

$$m_2 \ddot{y} + c_2 (\dot{y} - \dot{x}) + k_2 (y - x)^3 = 0 \quad (2)$$

Where  $m_1, c_1, k_1$  and  $m_2, c_2, k_2$  are the mass, damping and stiffness of the cutting tool and the NES respectively.  $F(\Delta h(t))$  is the non constant part of the cutting force expressed as:

$$F(\Delta h(t)) = a_p K_t (x(t - \tau) - x(t)) \quad (3)$$

Where  $a_p$  is the depth of cut,  $K_t$  is a cutting stiffness,  $x(t)$  is the current position of the tool and  $x_\tau = x(t - \tau)$  is the delayed position.  $\tau$  is the time delay which correspond to one workpiece revolution:

$$\tau = \frac{2\pi}{\Omega} \quad (4)$$

Where  $\Omega$  is the workpiece rotating speed.

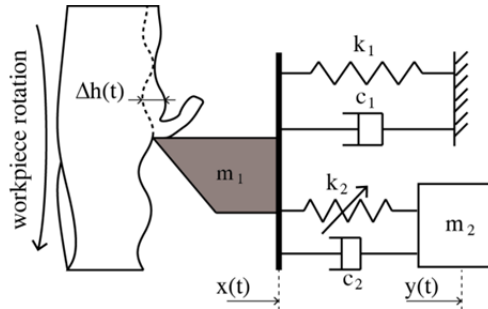


Figure 1: Scheme of the model

After rescaling, system (1,2) is rewritten in a more convenient form:

$$\ddot{x} + \lambda_1 \dot{x} + x + p(x - x_\tau) + \varepsilon \lambda_2 (\dot{x} - \dot{y}) + \varepsilon K(x - y)^3 = 0 \quad (5)$$

$$\ddot{y} + \lambda_2 (\dot{y} - \dot{x}) + K(y - x)^3 = 0 \quad (6)$$

With

$$\begin{aligned} \tilde{t} = \omega_1 t, \quad \varepsilon = m_2/m_1, \quad \omega_1^2 = k_1/m_1, \quad \omega_2^2 = k_2/m_2, \quad K = \omega_2^2/\omega_1^2, \\ \lambda_1 = c_1/(m_1\omega_1), \quad \lambda_2 = c_2/(m_2\omega_1), \quad p = a_p K_t / (m_1\omega_1^2), \quad \tilde{\tau} = \omega_1 \tau \end{aligned} \quad (7)$$

### 3. Equation of motion analysis

A new coordinate representing the internal displacement of the NES is introduced:

$$w = x - y \quad (8)$$

A new small parameter  $\chi$  is introduced, and the variables are rescaled as follows:

$$\chi = \varepsilon^{1/3}, \quad X = \chi^{-1}x, \quad W = w \quad (9)$$

Substituting (8,9) into (5,6), and keeping only terms up to order  $\chi^2$  yields:

$$\ddot{X} + X + \lambda_1 \dot{X} + p(X - X_\tau) + \chi^2 \lambda_2 \dot{W} + \chi^2 KW^3 = 0 \quad (10)$$

$$\ddot{W} + \chi X + \chi \lambda_1 \dot{X} + \chi p(X - X_\tau) + \lambda_2 \dot{W} + KW^3 = 0 \quad (11)$$

The system is analyzed in the case of 1:1 resonance. In this case all variables oscillate at the same frequency that is at the frequency of the bifurcated periodic orbit. System (10,11) may be reshaped as follows:

$$\ddot{X} + X + \lambda_1 \dot{X} + p(X - X_\tau) + \chi^2 \lambda_2 \dot{W} + \chi^2 KW^3 = 0 \quad (12)$$

$$\ddot{W} + \omega_c W + \chi \left[ \delta \left( \lambda_2 \dot{W} + KW^3 - \omega_c W \right) + X + \lambda_1 \dot{X} + p(X - X_\tau) \right] = 0 \quad (13)$$

Where  $\delta = \chi^{-1}$ . System (12,13) is the basis for the analysis. A detuning parameter representing the nearness of  $p$  to the critical value  $p_c$  is introduced as:

$$p = p_c + \chi^2 \sigma \quad (14)$$

System (12,13) is analyzed using the method of multiple scales. A second order uniform approximation of its solution in the vicinity of the Hopf bifurcation has the form:

$$X(t; \chi) = X_0(T_0, T_1, T_2) + \chi X_1(T_0, T_1, T_2) + \chi^2 X_2(T_0, T_1, T_2) + \dots \quad (15)$$

$$W(t; \chi) = W_0(T_0, T_1, T_2) + \chi W_1(T_0, T_1, T_2) + \chi^2 W_2(T_0, T_1, T_2) + \dots \quad (16)$$

Where  $T_n = \chi^n t$ ,  $n = 0, 1, \dots$ . The time delay term is expressed as:

$$X(t - \tau; \chi) = X_0(T_0 - \tau, T_1 - \chi\tau, T_2 - \chi^2\tau) + \chi X_1(T_0 - \tau, T_1 - \chi\tau, T_2 - \chi^2\tau) \\ + \chi^2 X_2(T_0 - \tau, T_1 - \chi\tau, T_2 - \chi^2\tau) + \dots \quad (17)$$

Substituting (15-17) into (12,13) and equating coefficients of like power of  $\chi$  yields:

$$D_0^2 X_0 + \lambda_1 D_0 X_0 + X_0 + p_c(X_0 - X_{0\tau}) = 0 \quad (18)$$

$$D_0^2 W_0 + \omega_c W_0 = 0 \quad (19)$$

$$D_0^2 X_1 + \lambda_1 D_0 X_1 + X_0 + p_c(X_1 - X_{1\tau}) = -2D_0 D_1 X_0 - \lambda_1 D_1 X_0 - p_c \tau D_1 X_{0\tau} \quad (20)$$

$$D_0^2 W_1 + \omega_c W_1 = -\delta \lambda_2 D_0 W_0 - \delta KW_0^3 + \delta \omega_c W_0 - X_0 + p_c(X_{0\tau} - X_0) - \lambda_1 D_0 X_0 - 2D_0 D_1 W_0 \quad (21)$$

$$D_0^2 X_2 + \lambda_1 D_0 X_2 + X_0 + p_c(X_2 - X_{2\tau}) = -2D_0 D_1 X_1 - D_1^2 X_0 + \frac{1}{2} p_c \tau^2 D_1^2 X_{0\tau} - p_c \tau D_2 X_{0\tau} \\ - p_c \tau D_1 X_{1\tau} + \sigma X_{0\tau} - 2D_0 D_2 X_0 - \lambda_1 D_1 X_1 - \lambda_1 D_2 X_0 - \sigma X_0 - KW_0^3 - \lambda_1 D_0 W_0 \quad (22)$$

Where  $X_{i\tau} = X_i(T_0 - \tau, T_1, T_2)$ . Only the equation governing the evolution of  $X_2$  is shown, because it is the only one used in this study. The general solution of Eq. (18) can be expressed as:

$$X_0 = A(T_1, T_2) e^{i\omega_c T_0} + \sum_{n=1}^{\infty} \left[ A_n(T_1, T_2) e^{(\gamma_n - i\omega_n) T_0} \right] + cc \quad (23)$$

Where  $cc$  stand for complex conjugate,  $\omega_c$  is the critical frequency of the oscillations on the boundary of Hopf bifurcation.  $(\gamma_n - i\omega_n)$  are the remaining roots of Eq. (18). Close to the Hopf bifurcation, all the roots have negative real parts except one which change sign at the stability boundary. After transient, all the roots decay with time, and the long time behavior at  $O(1)$  is given by:

$$X_0 = A(T_1, T_2) e^{i\omega_c T_0} + cc \tag{24}$$

$$W_0 = B(T_1, T_2) e^{i\omega_c T_0} + cc \tag{25}$$

Substituting (24,25) into (20,21) yields:

$$D_0^2 X_1 + \lambda_1 D_0 X_1 + X_0 + p_c (X_1 - X_{1\tau}) = (-2i\omega_c D_1 A - p_c \tau D_1 A - \lambda_1 D_1 A) e^{i\omega_c T_0} + cc \tag{26}$$

$$D_0^2 W_1 + \omega_c W_1 = (-\delta \lambda_2 B i \omega_c - 3\delta K B^2 B^* + \delta \omega_c B - A + p_c A e^{-i\omega_c \tau} - i\lambda_1 \omega_c A - p_c A - 2i\omega_c D_1 B) e^{i\omega_c T_0} + NST + cc \tag{27}$$

Where  $NST$  stands for non secular terms, and the star (\*) for the complex conjugate. Eliminating terms that produce secular terms in (26), one obtain:

$$A(T_1, T_2) = A(T_2) \tag{28}$$

Which means that  $A$  does not depend on time scale  $T_1$ , therefore:

$$X_0 = X_1 = A(T_2) e^{i\omega_c T_0} + cc \tag{29}$$

Now, eliminating terms that produce secular terms in (29) gives:

$$-\delta \lambda_2 i \omega_c B - 3\delta K B^2 B^* + \delta \omega_c B + p_c A e^{-i\omega_c \tau} - A - 2i\omega_c D_1 B - p_c A - \lambda_1 i \omega_c A = 0 \tag{30}$$

It is possible to prove with the help of Bendixon criterion, that a solution of (30) must end or begin at fixed point of the equation and cannot be periodic. Consequently, looking for the fixed points of (30):

$$\tilde{B}(T_2) = \lim_{T_1 \rightarrow \infty} B(T_1, T_2) \tag{31}$$

Then, one obtain:

$$A = - \frac{e^{i\omega_c \tau} \delta \tilde{B} (\lambda_2 i \omega_c + 3K |\tilde{B}|^2 - \omega_c)}{e^{i\omega_c \tau} (1 + p_c + i\lambda_1 \omega_c) - p_c} \tag{32}$$

The polar form is introduced as:

$$\tilde{B} = N e^{i\theta} \tag{33}$$

Substituting (33) into (32), and expressing  $A$  in terms of modulus yields:

$$|A|^2 = \delta^2 Z (\lambda_2^2 \omega_c^2 + \omega_c^2 + 9K^2 Z^2 - 6K Z \omega_c) \Gamma^{-1} \tag{34}$$

With

$$\Gamma = 1 + 2p_c + 2p_c^2 + 2p_c \lambda_1 \omega_c \sin(\omega_c \tau) + \lambda_1^2 \omega_c^2 - 2p_c^2 \cos(\omega_c \tau) - 2p_c \cos(\omega_c \tau) \tag{35}$$

And

$$N^2 = Z \tag{36}$$

Equation (34) defines the Slow Invariant Manifold (SIM) of the problem and inside its domain of attraction, variables  $A$  and  $B$  evolves on it. The SIM can be monotonous or have extremes. To verify this possibility, the roots of the derivative of the right hand side of (34) are computed:

$$Z_{1,2} = \frac{(2 \pm \sqrt{1 - 3\lambda_2^2}) \omega_c}{9K} \tag{37}$$

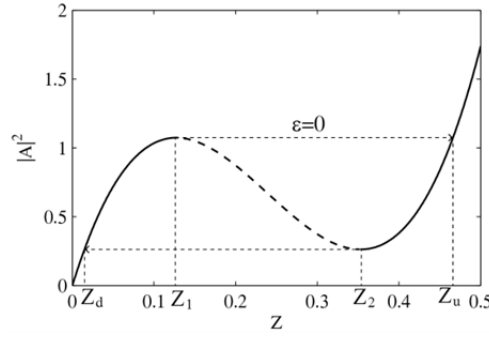


Figure 2: Shape of the SIM in the case  $\lambda_2 < 1/\sqrt{3}$ . Solid and dashed lines denotes stables and unstables branch respectively

Depending on the value of  $\lambda_2$ , the SIM can consist either of one stable branch if  $\lambda_2 > 1/\sqrt{3}$  or two stable and one unstable branch if  $\lambda_2 \leq 1/\sqrt{3}$ . In the later case, the structure of the SIM may give rise to relaxation oscillations. An example of such a SIM is presented in Fig.2. In the scenario of relaxation oscillation, also called Strongly Modulated Response (SMR), the flow can achieve fold points  $Z_1$  or  $Z_2$ , then the flow jump on the other stable branch to the landing point  $Z_u$  or  $Z_d$  respectively. These landing points are computed by using the invariance property of the SIM:

$$\delta^2 Z_{1,2} (\lambda_2^2 \omega_c^2 + \omega_c^2 + 9K^2 Z_{1,2}^2 - 6K Z_{1,2} \omega_c) = \delta^2 Z_{u,d} (\lambda_2^2 \omega_c^2 + \omega_c^2 + 9K^2 Z_{u,d}^2 - 6K Z_{u,d} \omega_c) \quad (38)$$

Then

$$Z_{u,d} = \frac{(1 \pm \sqrt{1 - 3\lambda_2^2}) 2\omega_c}{9K} \quad (39)$$

To study the different response regimes on the SIM, the equation at  $O(\chi^2)$  should be analysed. Substituting (25) and (29) into (22) yields to the following equation:

$$\begin{aligned} & D_0^2 X_2 + \lambda_1 D_0 X_2 + X_0 + p_c (X_2 - X_{2\tau}) \\ &= -p_c \tau D_2 A e^{-i\omega_c \tau} + \sigma A e^{-i\omega_c \tau} - \lambda_2 i \omega_c B - \lambda_1 D_2 A \\ & \quad - \sigma A - 3K B^2 B^* - 2i\omega_c D_2 A + NST + cc \end{aligned} \quad (40)$$

Eliminating terms that produce secular terms in (40) gives:

$$-p_c \tau D_2 A e^{-i\omega_c \tau} + \sigma A e^{-i\omega_c \tau} - \lambda_2 i \omega_c B - \lambda_1 D_2 A - \sigma A - 3K B^2 B^* - 2i\omega_c D_2 A = 0 \quad (41)$$

The equation for the SIM (34) is substituted into (41). Splitting into real and imaginary parts, and reorganizing, it is possible to obtain an expression for the derivative of  $N$ . The entire expression is not displayed here due to its length, but it can be expressed in more compact form as:

$$D_2 N = \frac{N (\alpha_1 N^4 + \alpha_2 N^2 + \alpha_3)}{\beta_1 N^4 + \beta_2 N^2 + \beta_3} \quad (42)$$

Where  $\alpha_i$  and  $\beta_i$  are coefficients which depends only on the systems parameters. The behavior of the system can be understood by studying the fixed points of (42). From (42), it follows that a trivial fixed point is  $N_0=0$  and the two others are expressed as:

$$Z_0 = \frac{-\alpha_2 \pm \sqrt{\alpha_2^2 - 4\alpha_1 \alpha_3}}{2\alpha_1} \quad (43)$$

#### 4. Description of some response regimes

In this section, some different response regimes are studied. The following set of parameters has been used for each cases:

$$\varepsilon = 0.01, \quad \lambda_1 = 0.1, \quad \lambda_2 = 0.2, \quad K = 1, \quad p_c = 0.12, \quad \tau = 3.94, \quad \omega_c = 1.08 \quad (44)$$

Only the detuning parameter  $\sigma$ , which can be related to the depth of cut, will varies. Initial conditions used for simulation are  $x(0) = 0.1$  and  $\dot{x}(0) = w(0) = \dot{w}(0) = 0$ . The integration scheme used for numerical simulation is the Matlab dde23 algorithm. The stable fixed points on the SIM are denoted by circles, and the unstable one by cross. The NES is not optimized in this study.

#### 4.1. Complete suppression of chatter

In Fig. 3, the SIM for  $\sigma = 0.05$  is presented. In this case, a stable fixed point exists at the origin, and an unstable one on the second stable branch of the SIM. In this case, the flow is repelled to the origin, and chatter is fully suppressed. This scenario is confirmed by numerical integration.

One can see that the oscillations decrease slowly to a value close to zero. It is not presented here, but for higher initial conditions (initial conditions on the second stable branch of the SIM), the flow will jump down to the first stable branch of the SIM as illustrated by the arrows on Fig. 2, and energy pumping occurs. Numerically, we have found that such a scenario occurs for  $\sigma < 0.052$ . For higher values of  $\sigma$ , other mechanisms are observed.

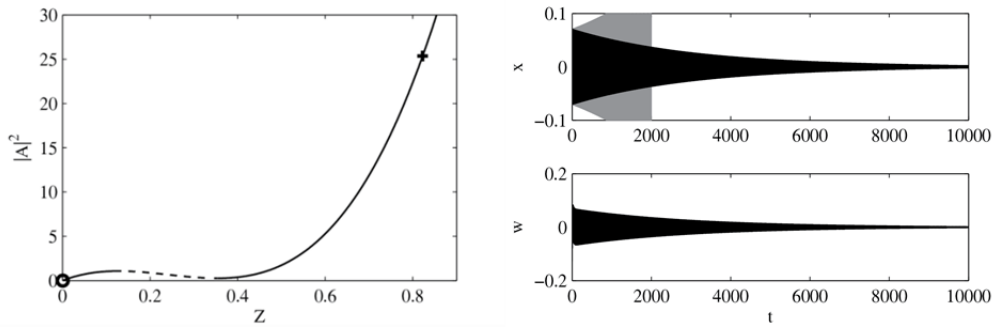


Figure 3: Case of complete suppression of chatter for the set of parameters (44) and  $\sigma = 0.05$ . Left: Structure of the SIM. 'o' and '+' denotes stable and unstable. Right: Numerical verification; black line : coupled system, gray line: uncoupled system fixed points respectively

#### 4.2. Stabilization of chatter

In Fig. 4, the SIM is presented for a slightly higher value of detuning parameter:  $\sigma = 0.09$ . Now the only stable fixed point is located on the first stable branch of the SIM and corresponds to small oscillations amplitude. Numerical verification is also presented. The amplitude of oscillation growth slowly and stabilize at the fixed point. This scenario occurs until the fixed point reaches the fold point  $Z_f$  (see Fig. 2).

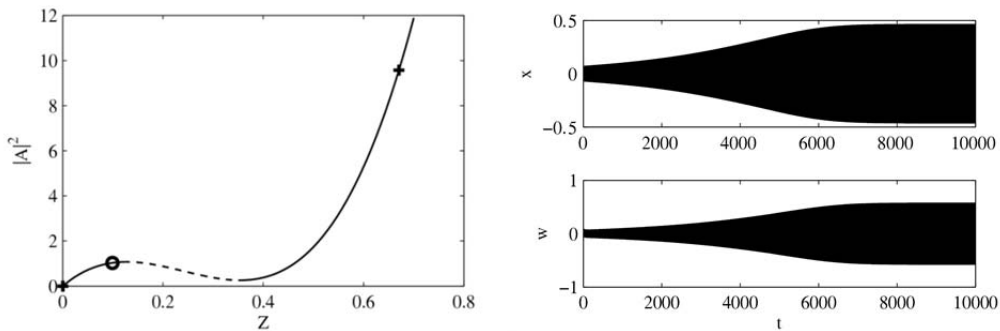


Figure 4: Case of stabilization of chatter for the set of parameters (44) and  $\sigma = 0.09$ . Left: Structure of the SIM. 'o' and '+' denotes stable and unstable. Right: Numerical verification

### 4.3. Chatter control through SMR

Further increase of  $\sigma$ , brings the possibility of appearance of SMR. As it is illustrated on the SIM in Fig. 5 for  $\sigma=0.2$ , there exist two unstable fixed points on each stable branch of the SIM, and another unstable fixed point on the unstable branch of the SIM. In this case, the only way for the flow is to perform relaxation cycle oscillations called SMR response. This regime is also verified numerically. It is interesting to find the value of  $\sigma$  for which SMR appears. This arises when the fixed point on the first stable branch of the SIM reaches the first fold point  $Z_I$ . The value of  $\sigma$  where this transition occurs was  $\sigma = 0.120$  numerically, versus  $\sigma = 0.111$  analytically. This is in good agreement despite the fact that the parameter  $\chi$  is not very small ( $\chi = 0.215$ ).

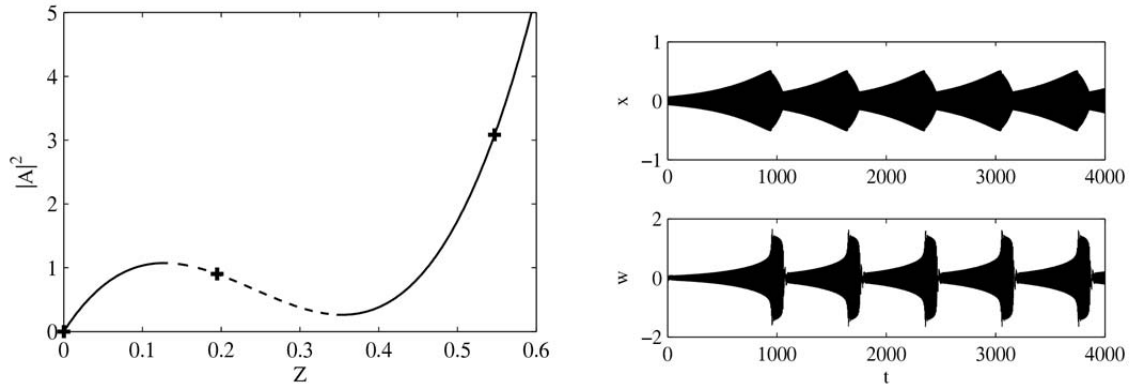


Figure 5: Case of passive control of chatter via SMR for the set of parameters (44) and  $\sigma = 0.2$ . Left: Structure of the SIM. 'o' and '+' denotes stable and unstable. Right: Numerical verification

### 4.4. Loss of stability

Again increasing the value of  $\sigma$ , the fixed point located on the second stable branch of the SIM goes down until it reaches the saddle point  $Z_u$  yielding to an homoclinic connection. A slightly increase of  $\sigma$ , makes system unstable. In this case, with initial conditions on the first branch of the SIM, the flow must grow on this branch until the fold point  $Z_I$ , then land on the second stable branch, and increase infinitely (unstable). This is fully verified in Fig. 6, where the motion becomes unstable after one half SMR cycle. Numerically, the value of  $\sigma$  where SMR loss stability is  $\sigma = 0.409$  versus  $\sigma = 0.455$  analytically.

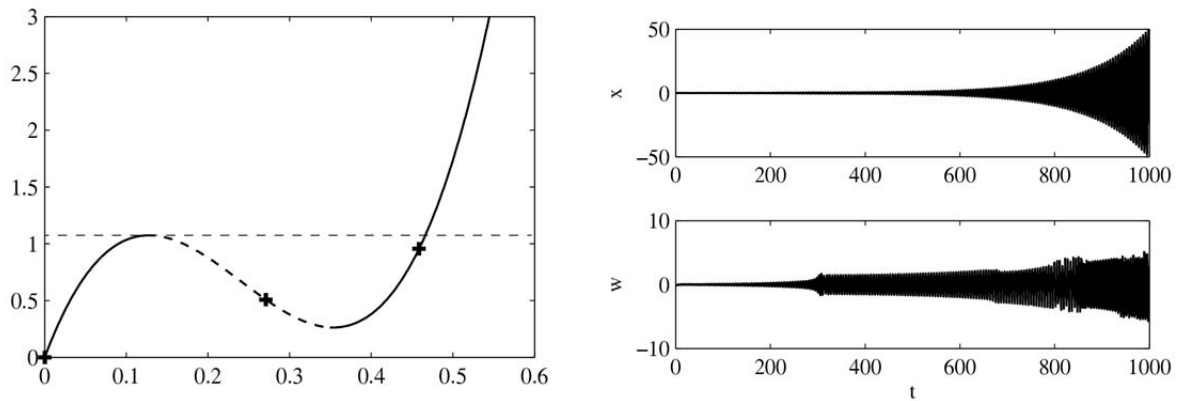


Figure 6: Loss of stability for the set of parameters (44) and  $\sigma = 0.5$ . Left: Structure of the SIM. 'o' and '+' denotes stable and unstable. Right: Numerical verification



## 5. Conclusion

In this paper, the possibility of passively controlling machining chatter instability with a nonlinear energy sink was studied. The system considered consists of a linear oscillator representing a flexible lathe cutting tool, subject to a regenerative cutting force and strongly coupled to a NES. Only the linear part of the cutting force was considered. The whole system has been studied using the method of multiple scales. Different responses regimes were revealed by studying the location of the fixed points on the SIM. Qualitatively, the comparison between analytical prediction and numerical simulation is very satisfying. Quantitatively, some discrepancies arise in the determination of the critical parameters, certainly due to the not so small value of  $\chi$ . The potential benefit of the NES to control machining chatter has been demonstrated. It should be interesting to include a non-linear cutting law, and to study the system's behavior for a larger set of parameters and an optimized NES in a further study.

## References

1. S.A. Tobias and W. Fishwick. Theory of regenerative machine tool chatter. *Eng.* 205:199–203, 1958.
2. B.P. Mann, T. Insperger, G. Stepan, and P.V. Bayly. Stability of up-milling and down-milling, part 2: experimental verification. *Int. J. Mach. Tools Manuf.* 43:35–40, 2003.
3. E. Gourc, S. Seguy, and L. Arnaud. Chatter milling modeling of active magnetic bearing spindle in high-speed domain. *Int. J. Mach. Tools Manuf.* 51:928–936, 2011.
4. A.H. Nayfeh and N.A. Nayfeh. Analysis of the cutting tool on a lathe. *Nonlinear Dyn.* 63:395–416, 2010.
5. S. Seguy, T. Insperger, L. Arnaud, G. Dessein, and G. Peigne. Suppression of period doubling chatter in high-speed milling by spindle speed variation. *Mach Sci Technol*, 15:153–171, 2011.
6. N.D. Sims. Vibration absorbers for chatter suppression: a new analytical tuning methodology. *J. Sound Vib.* 301:592–607, 2007.
7. H. Moradi, F. Bakhtiari-Nejad, and M.R. Movahhedy. Tuneable vibration absorber design to suppress vibrations: an application in boring manufacturing process. *J. Sound Vib.* 318:93–108, 2008.
8. A. Harms, B. Denkena, and N. Lhermet. Tool adaptator for active vibration control in turning operations. In 9th International Conference on New Actuators, Brême, Germany, 2004.
9. M. Wang. Feasibility study of nonlinear tuned mass damper for machining chatter suppression. *J. Sound Vib.* 330:1917–1930, 2011.
10. O.V. Gendelman, E. Gourdon, and C.H. Lamarque. Quasiperiodic energy pumping in coupled oscillators under periodic forcing. *J. Sound Vib.* 294(4-5):651–662, 2006.
11. A.F. Vakakis and R.H. Rand. Non-linear dynamics of a system of coupled oscillators with essential stiffness non-linearities. *Int. J. Non-linear Mech.* 39(7):1079 – 1091, 2004.
12. O.V. Gendelman. Bifurcations of nonlinear normal modes of linear oscillator with strongly nonlinear damped attachment. *Nonlinear Dyn.* 37:115– 128, 2004.
13. A. Nankali, H. Surampalli, Y.S. Lee, and T. Kalmar-Nagy. Suppression of machine tool chatter using non-linear energy sink. Proceedings of ASME-IDE/TC, Washington DC, USA, 2011.
14. Y. Starosvetsky and O.V. Gendelman. Strongly modulated response in forced 2dof oscillatory system with essential mass and potential asymmetry. *Physica D.* 237(13):1719–1733, 2008.